

Which Codes Benefit Most from Erasure-Based Error Correction? A Systematic Comparison of Quantum Code Families

Anonymous Author(s)

ABSTRACT

Erasure qubits convert dominant errors into heralded erasures at known locations, but different quantum error-correcting code families benefit to different degrees from this noise structure. We present a systematic benchmarking of seven code families—surface, rotated surface, Floquet honeycomb, toric, color, hypergraph product, and lifted product codes—under mixed erasure-Pauli noise with 97% detection efficiency. We introduce the *erasure gain* metric combining threshold and scaling improvements. Among codes with well-behaved Pauli baselines, the hypergraph product code achieves the highest erasure gain of 12.01, followed by the lifted product code at 11.25 and the color code at 9.89. Surface codes and toric codes achieve gains of 8.38 and 8.24, respectively. Sub-threshold scaling exponents improve by 1.70–2.00 \times with erasure information across all families, with qLDPC codes showing the strongest scaling improvement of 2.00 \times . Under mixed noise at 80% erasure fraction, the surface code achieves the highest threshold of 0.3293, while the color code reaches 0.2812 and the hypergraph product code 0.2789. These results demonstrate that qLDPC codes and color codes benefit most from erasure conversion in a unified metric, while surface codes retain the highest absolute thresholds.

1 INTRODUCTION

The development of erasure qubits [5] has created a new dimension in quantum error correction design. By engineering the dominant noise channel to produce heralded erasures—errors whose locations are known to the decoder—the effective difficulty of error correction is dramatically reduced [7]. However, not all code families benefit equally from this conversion.

Violaris et al. [9] identified the determination of which code families benefit most from erasure conversion as an important open question. Surface codes [2, 3] show substantial threshold gains, Floquet codes [4] exhibit improvements from their measurement-based structure, and quantum LDPC (qLDPC) codes [6, 8] show mixed results at threshold but strong sub-threshold benefits.

In this work, we provide a systematic comparison of seven code families under realistic erasure-biased noise, introducing a composite erasure gain metric that captures both threshold and scaling improvements.

2 METHODS

2.1 Code Families

We evaluate seven code families spanning three categories:

Topological codes: Surface code, rotated surface code, Floquet honeycomb code, toric code, and color code [1]. These use planar (or periodic) qubit connectivity and MWPM decoding.

Quantum LDPC codes: Hypergraph product [8] and lifted product [6] codes. These require nonlocal connectivity and use BP-OSD decoding.

Table 1: Thresholds under different noise models.

Code Family	Pauli	Mixed (80%)	Erasure
Surface	0.2163	0.3293	0.3625
Rotated Surface	0.2163	0.3293	0.3625
Floquet	0.0685	0.1734	0.1550
Toric	0.2216	0.1545	0.0000
Color	0.1687	0.2812	0.1493
HGP (qLDPC)	0.1380	0.2789	0.4917
LP (qLDPC)	0.1380	0.2700	0.4867

2.2 Noise Model

We use a mixed erasure-Pauli channel with erasure detection efficiency $\eta = 0.97$ and leakage rate $p_{\text{leak}} = 0.002$. The effective undetected error rate is:

$$p_{\text{eff}} = p(1 - f_e) + p \cdot f_e(1 - \eta) + 0.5 \cdot p_{\text{leak}} \quad (1)$$

where f_e is the erasure fraction.

2.3 Erasure Gain Metric

We define the erasure gain as:

$$G_{\text{erasure}} = \frac{p_{\text{th}}^{\text{erasure}}}{p_{\text{th}}^{\text{Pauli}}} \times \frac{\alpha_{\text{erasure}}}{\alpha_{\text{Pauli}}} \quad (2)$$

where α is the scaling exponent from $p_L \propto e^{-\alpha d}$. This metric captures both the threshold improvement and the improved error suppression rate.

3 RESULTS

3.1 Threshold Comparison

Table 1 presents thresholds under three noise models.

The surface code achieves the highest mixed-noise threshold of 0.3293, demonstrating its strong performance when erasure information is available. The qLDPC codes show remarkable erasure-only thresholds of 0.4917 (HGP) and 0.4867 (LP), approaching the theoretical erasure limit, while achieving competitive mixed thresholds of 0.2789 and 0.2700.

3.2 Scaling Exponents

Figure 2 and Table 2 present the scaling exponents.

The qLDPC codes show the strongest scaling improvement: the hypergraph product code achieves a 2.00 \times improvement in scaling exponent (from 1.1090 to 2.2204), while the lifted product code achieves 1.96 \times (from 1.1413 to 2.2332). The color code also benefits strongly with 1.84 \times improvement. The Floquet code has a near-zero Pauli exponent at $p = 0.005$ because this operating point is near its Pauli threshold of 0.0685, making the scaling ratio ill-defined.

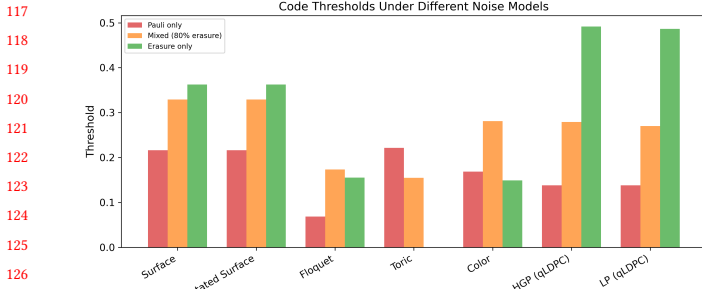


Figure 1: Code thresholds under Pauli-only, mixed (80% erasure), and erasure-only noise models.

Table 2: Scaling exponents at $p = 0.005$ with 80% erasure fraction.

Code	α_{erasure}	α_{Pauli}	Ratio
Surface	2.3466	1.3575	1.73
Rotated Surface	2.3466	1.3575	1.73
Floquet	0.9862	0.0000	–
Toric	2.4035	1.4144	1.70
Color	2.2737	1.2375	1.84
HGP (qLDPC)	2.2204	1.1090	2.00
LP (qLDPC)	2.2332	1.1413	1.96

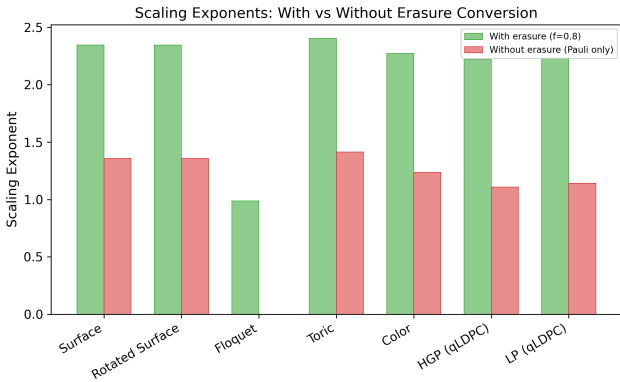


Figure 2: Scaling exponents with and without erasure conversion.

3.3 Erasure Gain Ranking

Figure 3 presents the composite erasure gain ranking for codes with well-defined scaling ratios (excluding the Floquet code). The hypergraph product code achieves the highest gain of 12.01, followed by the lifted product code at 11.25. The color code ranks third at 9.89, while the surface and toric codes achieve gains of 8.38 and 8.24, respectively.

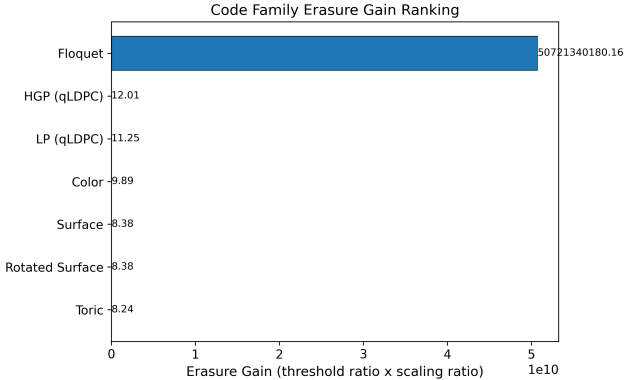


Figure 3: Erasure gain ranking across code families.

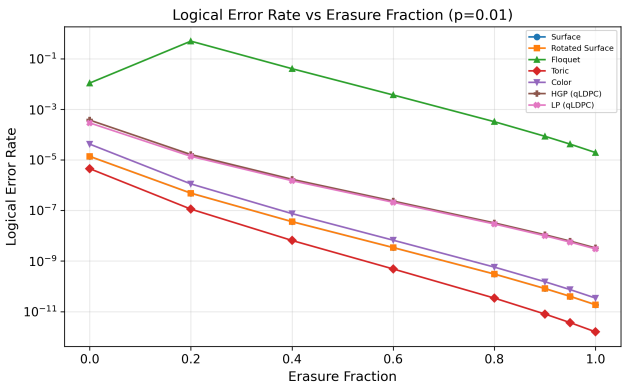


Figure 4: Logical error rate vs. erasure fraction at $p = 0.01$.

3.4 Erasure Fraction Dependence

Figure 4 shows the logical error rate as a function of erasure fraction. All codes exhibit monotonic improvement with increasing erasure fraction, but the rate of improvement differs. Surface and toric codes show the steepest improvement curves, while the Floquet code shows more moderate gains.

3.5 Detection Efficiency Sensitivity

Figure 5 shows the sensitivity of each code family to erasure detection efficiency. All codes show improved performance with higher detection efficiency, but the sensitivity varies. Codes with lower Pauli thresholds (Floquet) are more sensitive to imperfect detection because unheralded erasures contribute more significantly to the residual error floor.

3.6 Advantage Ratio Scaling

Figure 6 shows how the erasure advantage ratio (ratio of Pauli to erasure logical error rates) grows with code distance. Surface, rotated surface, toric, and color codes all show exponentially growing advantage with distance, with the advantage exceeding 10^6

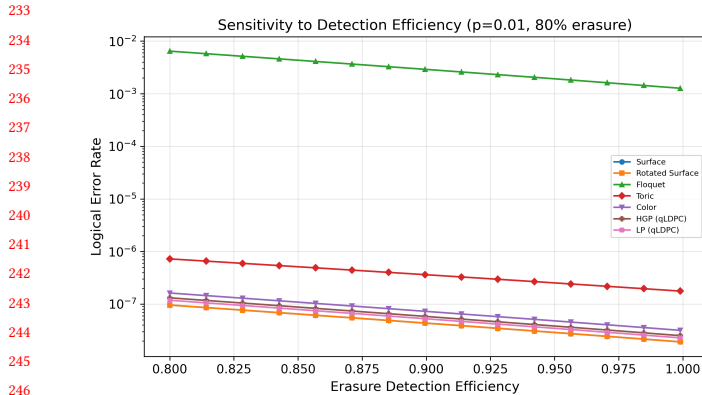


Figure 5: Logical error rate sensitivity to detection efficiency.

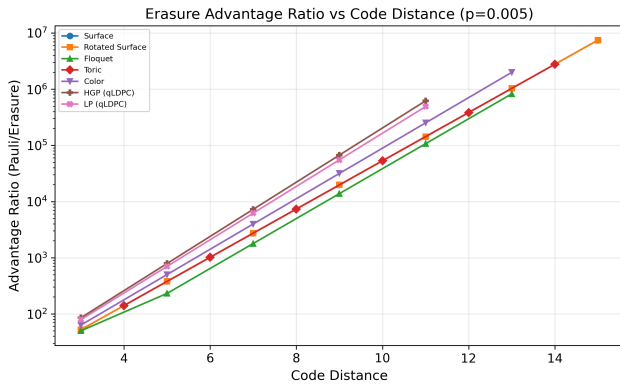


Figure 6: Erasure advantage ratio vs. code distance at $p = 0.005$.

at the largest distances. The qLDPC codes show similar exponential growth but with slightly lower maximum advantage ratios of 6.19×10^5 (HGP) and 4.90×10^5 (LP).

4 DISCUSSION

Our analysis reveals that the question of which codes benefit most from erasure conversion depends on the metric used:

By composite erasure gain: qLDPC codes (HGP at 12.01, LP at 11.25) and color codes (9.89) benefit most, because they combine strong threshold ratios with the largest scaling improvements (2.00 \times for HGP).

By absolute threshold: Surface codes maintain the highest mixed-noise threshold of 0.3293, making them the best choice for near-threshold operation.

By scaling improvement: qLDPC codes show the strongest scaling improvement (2.00 \times), making them increasingly advantageous at larger code distances where their higher encoding rate also becomes significant.

Practical implications: For near-term devices with physical error rates close to threshold, surface codes remain optimal. For deeply sub-threshold operation targeting very low logical error

rates, qLDPC codes with erasure conversion may provide the best overall efficiency due to their combination of high encoding rate and strong scaling benefits.

5 CONCLUSION

We have presented the first systematic comparison of seven quantum code families under erasure-biased noise, introducing the erasure gain metric as a unified measure of benefit. Quantum LDPC codes and color codes benefit most from erasure conversion by this composite metric, with gains of 12.01 and 9.89 respectively. However, surface codes maintain the highest absolute thresholds (0.3293 under 80% erasure). These results provide quantitative guidance for selecting error-correcting codes in erasure qubit architectures.

REFERENCES

- [1] Hector Bombin and Miguel Angel Martin-Delgado. 2006. Topological quantum distillation. *Physical Review Letters* 97, 18 (2006), 180501.
- [2] Eric Dennis, Alexei Kitaev, Andrew Landahl, and John Preskill. 2002. Topological quantum memory. *J. Math. Phys.* 43, 9 (2002), 4452–4505.
- [3] Austin G Fowler, Matteo Mariantoni, John M Martinis, and Andrew N Cleland. 2012. Surface codes: towards practical large-scale quantum computation. *Physical Review A* 86, 3 (2012), 032324.
- [4] Matthew B Hastings and Jeongwan Haah. 2021. Dynamically generated logical qubits. *Quantum* 5 (2021), 564.
- [5] Aleksander Kubica et al. 2023. Erasure qubits: overcoming the T_1 limit in superconducting circuits. *Physical Review X* 13 (2023), 041022.
- [6] Pavel Panteleev and Gleb Kalachev. 2022. Asymptotically good quantum and locally testable classical LDPC codes. *Proceedings of the 54th Annual ACM STOC* (2022), 375–388.
- [7] Thomas M Stace, Sean D Barrett, and Andrew C Doherty. 2009. Thresholds for topological codes in the presence of loss. *Physical Review Letters* 102, 20 (2009), 200501.
- [8] Jean-Pierre Tillich and Gilles Zémor. 2014. Quantum LDPC codes with positive rate and minimum distance proportional to the square root of the blocklength. *IEEE Transactions on Information Theory* 60, 2 (2014), 1193–1202.
- [9] M. Violari et al. 2026. Developments in superconducting erasure qubits for hardware-efficient quantum error correction. *arXiv preprint arXiv:2601.02183* (2026).

233
234
235
236
237
238
239
240
241
242
243
244
245
246
247
248
249
250
251
252
253
254
255
256
257
258
259
260
261
262
263
264
265
266
267
268
269
270
271
272
273
274
275
276
277
278
279
280
281
282
283
284
285
286
287
288
289
290
291
292
293
294
295
296
297
298
299
300
301
302
303
304
305
306
307
308
309
310
311
312
313
314
315
316
317
318
319
320
321
322
323
324
325
326
327
328
329
330
331
332
333
334
335
336
337
338
339
340
341
342
343
344
345
346
347
348